Two Highly Populated Conformations at Room Temperature of Monterine and Granjine, Antitumor Bisbenzylisoquinoline Alkaloids: Origin and Tridimensional Structures

Akino Jossang,*[,†] Adrien Cavé,[‡] Jairo Saez,[§] Marie Hélène Bartoli,[||] André Cavé,[⊥] and Per Jossang[†]

Laboratoire de Chimie, CNRS URA 401, Muséum National d'Histoire Naturelle, 63 rue Buffon 75005 Paris, France; Centre de Biochimie Structurale, CNRS UMR C9955, INSERM U414, Université Montpellier I, 34060 Montpellier, France; Departamento de Quimica, Universidad de Antioquia, AA 1226 Medellin, Colombia; Laboratoire de Pharmacie Clinique et de Biotechnique (GREPO), UFR de Pharmacie de Grenoble, 38700 La Tronche, France; and Laboratoire de Pharmacognosie, CNRS URA 1843, Faculté de Pharmacie, Université de Paris XI, 92296 Châtenay-Malabry Cedex, France

Received April 24, 1995 (Revised Manuscript Received February 22, 1996[⊗])

Monterine **1** as well as granjine **3**, 1*R*,1′*S* configured biphenylic bisbenzylisoquinoline alkaloids, generate two highly populated conformers. The interconversion of two forms was detected by saturation tranfer in ^{1}H NMR NOEs experiments. Tridimensional structure of the conformers was determined on the basis of ^{1}H NMR analysis of anisotropic shielding protons, by NOEs measurements and vicinal proton coupling constants of CH1−CH$_2$α and CH1′−CH$_2$α′. The structures established from NMR data were further refined to observe the mobility of 3D conformations by molecular dynamics simulation *in vacuo*. The highly populated conformers, monterine **1a** and **1b,** as well as granjine **3a** and **3b,** are interconvertible by rotation about the C1′−Cα′, Cα′−C9′, and C11′−C11 bonds and inversion of the benzyl D ring by reference to CH$_2$α′. The slow exchange system was investigated by dynamic NMR spectroscopy: $\Delta G^{\ddagger}_c$ 77.9 KJ/mol and k_c 200 s^{-1} for monterine **1**; $\Delta G^{\ddagger}_c$ 77.7 KJ/mol and k_c 211 s^{-1} for granjine **3**. Natural and synthetic biphenylic bisbenzylisoquinolines displayed, *in vitro*, cytotoxic activities against human prostate and breast cancer cell lines.

The bisbenzylisoquinoline alkaloids isolated from plants encompass a number of compounds[1−4] distributed among 27 structural groups.[1,5] They exhibit a broad spectrum of biological activities (muscle relaxant, antitumor, antibacterial, antimalarial, cardiovascular, and immunomodulatory effects and others).[2−4] In view of establishing structure−activity relationships, knowledge of tridimensional structure and conformational characteristics are of great interest.

In the group of bisbenzylisoquinolines connected by two ether bonds, C8−O−C7′ and C11−O−C12′, synthetic 1′,2′-dehydronorphaeanthine[6] (natural dehatrine)[7] and thalisimine[8] were reported to present, at room temperature, double signals in the ^{1}H NMR spectra, due to the existence of two conformers. Doubling of ^{13}C NMR signals was also reported for oxyacanthine and obaberine in another group (1*S*,1′*R*) of bisbenzylisoquinolines with two ether bonds C7−O−C8′ and C11−O−C12′.[9] The effect was found in dimethyl- and diacetyl-antioquine[10] and dimethylpseudoxandrine (1*S*,1′*R*),[11] too, bisbenzylisoquinolines linked by an ether C8−O−C7′ bond and a biphenylic C11−C11′ bond. Owing to the complex NMR spectra, complete assignment was difficult. Some cyclic compounds such as benzodiazepinones, thiazolinethiones, cyclophanes, and cycloalkenes are also known to present two sets of heat coalescing NMR signals at room temperature.[12,13]

We previously noticed the presence, in solution, of two conformers of monterine **1** and granjine **3**, isolated from a Crematosperma species.[14] We present herein an investigation of the origin of the highly populated conformers: monterine **1** and granjine **3**, 16-membered macrolide bisbenzylisoquinoline alkaloids, and a construction of their possible tridimensional structures on the basis of NMR data and comparison with those obtained by molecular dynamic simulation calculations. The exchange system was examined by dynamic NMR spectroscopy. Antitumor activity of these and related alkaloids is also discussed.

† Muséum National d'Histoire Naturelle.
‡ Centre de Biochimie Structurale, Montpellier.
§ Universidad de Antioquia.
|| Faculté de Pharmacie, Grenoble.
⊥ Faculté de Pharmacie, Châtenay-Malabry.
⊗ Abstract published in *Advance ACS Abstracts,* April 15, 1996.

(1) Guha, K. P.; Mukherjee, B.; Mukherjee, R. *J. Nat. Prod.* **1979**, *42*, 1, and references therein.
(2) (a) Schiff, P. L., Jr. *J. Nat. Prod.* **1983**, *46*, 1−43. (b) *Ibid.* **1987**, *50*, 529, and references therein.
(3) Buck, K. J. The Bisbenzylisoquinoline Alkaloids. in *The Alkaloids*; Brossi, A. ed., Academic Press: New York, 1987; Vol. 30, pp 1−222.
(4) Schiff, P. L., Jr. *J. Nat. Prod.* **1991**, *54*, 645, and references therein.
(5) Jossang, A.; Leboeuf, M.; Cavé, A.; Sévenet, T. *J. Nat. Prod.* **1986**, *49*, 1028.
(6) Inubushi,Y.; Masaki, Y.; Matsumoto, S.; Takami, F. *Tetrahedron Lett.* **1968**, 3399. Inubushi,Y.; Masaki, Y.; Matsumoto, S.; Takami, F. *J. Chem. Soc.* (C) **1969**, 1547.
(7) Lu, S. T.; Tsai, I. L.; Leou, S.-P. *Phytochemistry* **1989**, *28*, 615. Kitagawa, I.; Minagawa, K.; Zhang, R.; Hori, K.; Doi, M.; Inoue, M.; Ishida, T.; Kimura, M.; Uji, T.; Shibuya, H. *Chem. Pharm. Bull.* **1993**, *41*, 997.
(8) Saa, J. M.; Lakshmikantham, M. V.; Mitchell, M. J.; Cava, M. P.; Beal, J. L.; Doskotch,R. W. *J. Org. Chem.* **1980**, *45*, 208.
(9) Ishii, H.; Kawanabe, E.; Seki, H.; Yamaguchi, K.; Akasu, A.; Kodama, K.; Kunitomo, J.-I. *Tennen Yuki Kagobutsu Toronkai Koen Yoshishu*, **1983**, *26*, 102; *Chem. Abstr.* **1984**, *100*, 156852y.
(10) Cortes, D.; Saez, J.; Hocquemiller, R.; Cavé, A.; Cavé, A. *J. Nat. Prod.* **1985**, *48*, 76.
(11) Cortes, D.; Hocquemiller, R.; Cavé, A.; Saez, J.; Cavé, A. *Can. J. Chem.* **1986**, *64*, 1390.
(12) Marquardt, F. H. *J. Chem. Soc. B* **1971**, 366. Carter, R. E.; Drakenberg, T.; Roussel, C. *J. Chem. Soc., Perkin Trans. 2* **1975**, 1690. Marshall, J. A.; Konicek, T. R.; Flynn, K. E. *J. Am. Chem. Soc.* **1980**, *102*, 3287. Sakamoto, K.; Ôki, M. *Bull. Chem. Soc. Jpn.* **1975**, *48*, 497.
(13) Ôki, M; *Application of Dynamic NMR Spectroscopy to Organic Chemistry*; VCH Publishers: New York, 1985.
(14) Saez, J.; Fernandez, E.; Jossang, A.; Cavé, A.; Cavé, A. *Can. J. Chem.* **1989**, *67*, 275.

S0022-3263(95)00767-5 CCC: $12.00

Chart 1

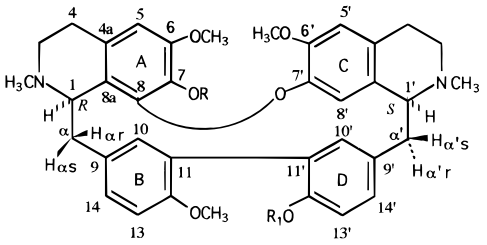

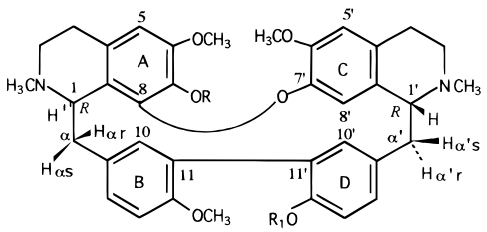

Monterine	**1**: R=H, R_1= CH_3	Epicordobine	**4**: R=R_1=H
Methylcordobine	**2**: R= CH_3, R_1=H	Epirodiasine	**5**: R= CH_3, R_1=H
Granjine	**3**: R=R_1=CH_3	Isogranjine	**6**: R=R_1=CH_3
Cordobine	**7**: R=R_1=H		

Results and Discussion

The first stage of this study surveyed structures in view of locating those presenting two sets of signals in the ^{1}H NMR spectrum, in the group of bisbenzylisoquinolines linked by biphenylic 11−11′ and ether 8−O−7′ bonds. Therefore, diverse O-methylated alkaloids were prepared. Epicordobine **4** was obtained from dihydrocordobimine 1′*R*[14] by N-methylation. Mild and selective 7-O-methylation produced epirodiasine **5** from alkaloid **4** and methylcordobine **2** from cordobine **7**.[14] Permethylation of compound **4** furnished isogranjine **6**. Among these alkaloids, only 1*R*,1′*S* configured monterine **1** and granjine **3** displayed double sets of signals in the ^{1}H and ^{13}C NMR spectra. In contrast, 7-*O*-methylcordobine **2** (1*R*, 1′*S*) and the alkaloids **4**, **5** as well as 12,12′-dimethoxylated **6**, possessing 1*R* and 1′*R* chiral centers, gave normal single ^{1}H and ^{13}C NMR spectra.

In the case of bisbenzylisoquinolines with biphenylic 11−11′ and ether C8−O−C7′ bonds, there is strong evidence that simultaneous presence of 12- and 12′-dimethoxy groups and 1*R*,1′*S* (or 1*S*,1′*R*) absolute configurations produce two highly populated conformations in solution, at 27 °C. The ratio of conformers **a** to **b** in $CDCl_3$ solution is 57/43 in monterine **1** and 70/30 in granjine **3**. The ratio is modified in pyridine-d_5 solution: 30/70 for compounds **1** and **3**.

^{1}H and ^{13}C resonances were assigned by analysis of 2D ^{1}H−^{1}H COSY, NOESY,[15] and 2D heteronuclear HMQC[16] and HMBC[17] spectra. Each of both species is described by two spin systems of three aromatic protons (δ 6.1−7.7), two spin systems of three aliphatic protons (δ 2.7−4.3), two spin systems of four aliphatic protons (δ 2.3−3.5), some singlets of *N*-methyl groups (δ 2.3−2.7) and *O*-methyl groups (δ 3.5−3.8), and three isolated aromatic protons (δ 6.1−6.5). The HMQC spectra are quite helpful to distinguish between vicinal and geminal proton signals in the CH_2CH_2 parts of tetrahydroisoquinoline ring. Resonance data are summarized in Tables 1 and 2.

NOEs Assignment and Saturation Transfer. The analysis of the NOESY spectra (600 MHz) as well as 1D NOE experiments affords two kinds of informations for complete assignments. The positive NOE responses of 1D experiments and the corresponding positive NOE cross peaks of 2D experiments give the information for linking spin systems previously observed. The negative cross peaks and the negative 1D responses to irradiation due to saturation transfer provide the information for establishing correspondence of two equivalent protons between conformers **1a** and **1b**, evidencing a slow exchange system on the NMR timescale.

The low-field part δ 3.4 to δ 7.8 of the ^{1}H NMR spectrum of monterine **1** is illustrated in trace 1 of Figure 1. At 300 K, irradiation of H1**a** at δ 4.31 produces saturation transfer[18] to H1**b** at δ 3.95 and yields 2 peaks assigned to H10**a** at δ 7.67 and H10**b** at δ 6.61 in the difference spectrum (Figure 1, trace 2) as well as 2 peaks of *N*-CH_3-2 **a** and **b** at δ 2.31 and δ 2.42 (not shown in the figure). At 275 K, saturation of H1**a** yields only H10**a**

Table 1. ^{1}H NMR Resonance Data, in $CDCl_3$ at 300 K (360 MHz)[a]

no.	1a	1b	2	3a	3b	4	5	6
H1 dd	4.31	3.95	4.07	4.32	3.90	4.10	4.17	3.98
Hα*s* dd	2.80	2.82	2.84	2.72	2.81	2.88	2.82	2.74
Hα*r* dd	3.08	2.98	3.14	3.11	3.03	3.00	2.93	2.98
J_{gem}	*14.0*	*14.0*	*14.0*	*15.1*	*14.5*	*14.1*	*14.1*	*15.0*
J_1,α*s*	*8.0*	*8.0*	*8.0*	*7.9*	*8.5*	*7.9*	*9.0*	*6.0*
J_1,α*r*	*<1.0*	*<1.0*	*<1.0*	*<1.0*	*<1.0*	*<1.0*	*3.0*	*<1.0*
H3 m	2.83	2.98	2.98	2.90	2.79	2.92	3.02	3.02
	3.25	3.53	3.44	3.56	3.27	3.42	3.44	3.44
H4 m	2.53	2.44	2.60	2.58	2.49	2.48	2.53	2.49
	2.54	2.94	2.94	2.97	2.98	2.96	2.94	2.98
H5 s	6.32	6.33	6.36	6.36	6.28	6.38	6.40	6.36
H10 d	7.67	6.61	7.30	7.66	6.62	7.62	7.58	7.56
H13 d	6.72	6.80	6.87	6.75	6.82	6.84	6.90	6.81
H14 dd	7.12	7.29	7.34	7.18	7.36	7.28	7.39	7.34
H1′ dd	3.56	3.79	3.76	3.63	3.82	3.69	3.75	3.62
Hα′*s* dd	2.70	3.30	2.95	2.78	3.28	3.02	2.70	2.62
Hα′*r* dd	3.11	2.92	3.16	3.11	2.98	3.15	3.07	3.17
J_{gem}	*12.4*	*13.0*	*12.6*	*12.9*	*13.7*	*14.1*	*14.0*	*13.0*
$J_{1'}$,α′*s*	*10.2*	*3.0*	*4.0*	*11.0*	*3.0*	*4.7*	*4.0*	*10.0*
$J_{1'}$,α′*r*	*5.0*	*4.0*	*8.0*	*3.5*	*5.2*	*4.1*	*4.0*	*3.0*
H3′ m	2.86	2.55	2.82	2.62	2.59	2.62	2.96	2.87
	3.36	2.95	3.30	3.35	2.98	3.07	3.34	3.28
H4′ m	2.74	2.47	2.73	2.72	2.47	2.56	2.58	2.68
	2.98	2.33	2.80	3.05	2.34	2.70	3.05	3.00
H5′ s	6.60	6.31	6.52	6.57	6.36	6.39	6.43	6.54
H8′ s	6.37	7.16	6.75	6.39	7.08	7.13	7.06	6.62
H10′ d	6.15	6.80	6.46	6.16	6.79	6.88	6.79	6.56
H13′ d	6.91	6.69	6.90	6.94	6.70	6.82	6.88	6.90
H14′ dd	7.21	7.21	7.25	7.27	7.23	7.26	7.30	7.25
NMe2 s	2.31	2.42	2.38	2.35	2.42	2.34	2.31	2.45
NMe2′ s	2.60	2.65	2.68	2.60	2.64	2.61	2.68	2.62
MeO6 s	3.79	3.82	3.80	3.76	3.78	3.82	3.80	3.77
MeO7 s	−	−	3.36	3.22	3.39	−	3.48	3.37
MeO12 s	3.75	3.77	3.84	3.72	3.73	3.86	3.86	3.73
MeO6′ s	3.50	3.46	3.50	3.49	3.44	3.32	3.36	3.33
MeO12′ s	3.81	3.72	−	3.80	3.69	−	−	3.75

[a] $J_{13,14}$ and $J_{13',14'}$: 8 Hz, $J_{10,14}$ and $J_{10',14'}$: 2 Hz.

(15) Kumar, A.; Ernst, R. R.; Wüthrich, K. *Biochem. Biophys. Res. Commun.* **1980**, *95*, 1. Macura, S.; Huang, Y.; Suter, D.; Ernst, R. R. *J. Magn. Reson.* **1981**, *43*, 259.

(16) Bax, A.; Subramanian, S. *J. Magn. Reson.* **1986**, *67*, 565.

(17) Bax, A.; Summers, M. F. *J. Am. Chem. Soc.* **1986**, *108*, 2093.

(18) Keller, R. M.; Wüthrich, K. *Biol. Magn. Reson.* **1981**, *3*, 1. Thanabal, V.; De Ropp, J. S.; La Mar, G. N. *J. Am. Chem. Soc.* **1987**, *109*, 265.

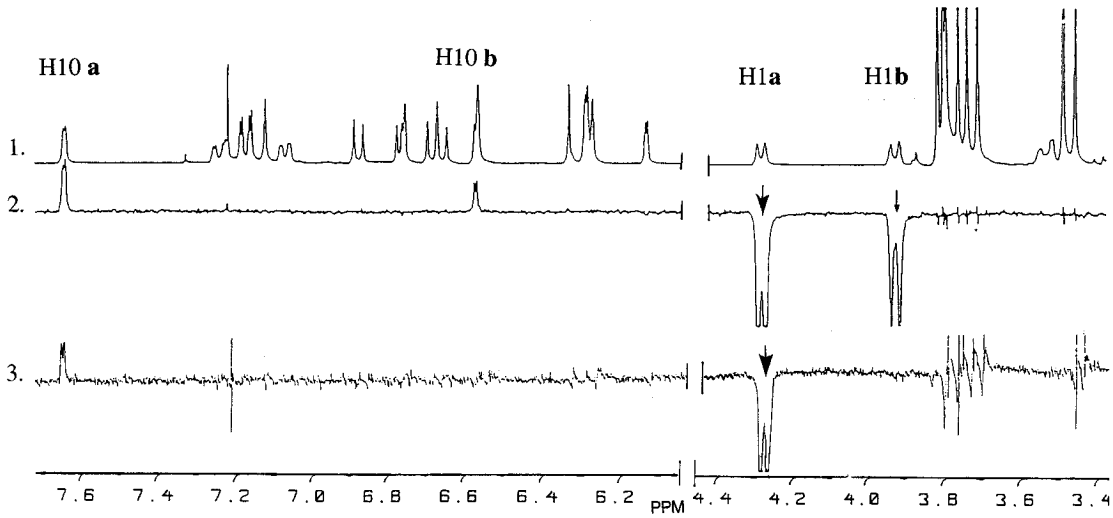

Figure 1. Selected NOEs and saturation transfer of monterine **1** at 300 K and 275 K in the δ 3.4−7.8. region. (1) The low-field part between δ 3.4 and δ 7.8 ppm of the 360-MHz ^{1}H NMR spectrum of monterine **1** ($CDCl_3$) at 300 K. (2) NOE, obtained at 300 K and upon saturation of the H1**a** signal, shows saturation transfer to H1**b** and subsequent enhancement of H10**a** and H10**b** together with 2 peaks of 2-*N*-CH_3 **a** and **b** at δ 2.27 and δ 2.39 (not shown in the figure). (3) NOE difference spectrum obtained at 275 K, saturation of H1**a** yields only H10**a** and 2-NCH_3**a** peaks, and no saturation transfer occurs.

Table 2. ^{13}C NMR Shifts ($CDCl_3$, * $CDCl_3$ + 5% CD_3OD, 300 K, 75 MHz)

carbon no.	1a	1b	2*	3a	3b	4*	5*	6
1	62.74	62.04	63.28	62.83	62.05	62.19	62.34	61.98
α	39.15	39.61	38.33	38.49	39.96	40.81	41.00	42.41
3	44.39	44.09	44.55	44.70	43.74	44.17	44.26	43.99
4	24.55	21.90	20.93	25.00	21.92	22.48	22.62	22.14
4a	122.56	122.90	125.63	129.63	130.09	124.53	127.35	127.85
5	104.40	104.40	105.54	105.30	105.51	105.41	106.40	106.10
6	146.24	146.09	151.30	150.91	151.01	146.20	151.58	151.24
7	141.36	142.10	137.10	135.98	137.22	136.03	138.79	138.54
8	147.57	147.57	147.30	147.36	148.10	142.35	148.62	148.82
8a	120.64	121.39	119.94	121.72	121.85	122.68	123.51	124.57
9	135.02	135.14	136.43	135.98	135.82	135.52	135.48	134.62
10	133.37	134.77	134.37	133.58	134.48	134.98	135.05	134.47
11	130.35	129.03	127.84	128.71	128.48	127.37	127.22	128.68
12	154.96	154.96	153.24	154.83	154.83	153.26	153.59	155.18
13	109.66	110.24	110.21	109.53	110.21	110.37	110.52	109.92
14	128.49	129.49	129.56	128.35	128.19	129.54	129.77	128.68
1′	64.57	64.57	64.38	64.66	64.66	64.70	64.74	64.87
α′	36.89	36.69	37.95	37.10	36.88	37.75	38.18	39.06
3′	44.91	51.33	44.55	44.77	51.65	44.17	44.26	44.74
4′	23.47	29.05	23.44	24.63	29.03	25.50	29.49	24.79
4′a	126.46	130.35	126.80	127.36	130.62	129.42	127.22	127.17
5′	112.43	111.63	112.35	112.29	111.34	113.59	113.35	113.49
6′	149.32	149.32	148.90	148.95	147.23	147.95	148.09	148.35
7′	141.84	143.40	141.80	141.20	143.25	143.11	143.34	143.15
8′	120.28	118.20	119.13	119.63	117.67	119.34	119.16	120.03
8′a	127.89	126.86	127.69	128.07	127.96	128.00	130.14	129.08
9′	134.49	134.49	136.43	130.09	128.13	130.46	128.47	130.46
10′	134.72	136.32	134.52	134.91	136.39	134.49	134.30	133.87
11′	128.77	128.29	129.13	127.36	126.47	125.37	125.49	127.95
12′	155.48	154.69	151.92	155.40	154.66	151.57	151.82	155.51
13′	110.93	109.51	116.75	111.01	112.29	116.60	116.78	110.89
14′	130.64	130.13	130.50	129.16	130.10	130.22	130.44	129.50
NMe2	42.30	41.86	41.75	42.69	41.99	41.74	41.67	41.66
NMe2′	41.40	43.86	41.99	42.14	44.06	42.48	42.17	41.78
MeO6	55.47	55.80	55.68	55.66	56.05	55.79	55.73	55.67
MeO7	−	−	60.20	60.25	60.04	−	60.14	60.08
MeO12	55.69	55.47	55.95	55.60	55.60	56.00	56.07	55.67
MeO6′	55.47	55.47	55.19	55.17	54.92	55.65	55.42	55.49
MeO12′	55.80	55.47	−	55.66	55.35	−	−	55.67

and NCH_3-2**a** peaks and no saturation transfer occurs (Figure 1, trace 3), thus the positive NOE becomes selective. The conformers **1a** and **1b** gave a negative cross peak in the NOESY[19] spectra at 300 K (Figure 2). These two sets of protons, in the 2D NOESY spectrum recorded at 300 K, were correlated by negative cross peaks corresponding to the same saturation transfer process. The 2D spectrum provides more complete information than 1D experiments. In a few cases, negative cross peaks cannot be observed due to the proximity of their chemical shifts as for Hαs**a** and Hαs**b**.

(19) Abel, E. W.; Coston, T. P. J.; Orrell, K. G.; Sik, V.; Stephenson, D. *J. Magn. Reson.* **1986**, *70*, 34.

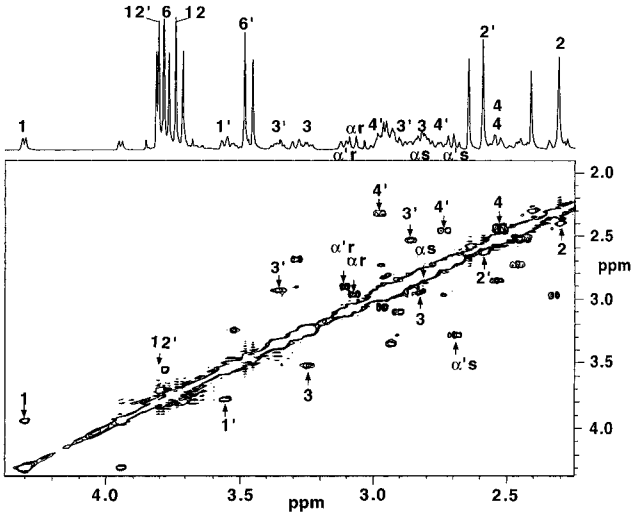

Figure 2. Negative NOESY spectrum of monterine **1** in high field recorded at 300 K and 600 MHz ($CDCl_3$). The negative cross peaks on the NOESY spectrum establish interconversion of two equivalent protons of conformers **1a** and **1b**. The labeled chemical shifts belong to the major conformer **1a**.

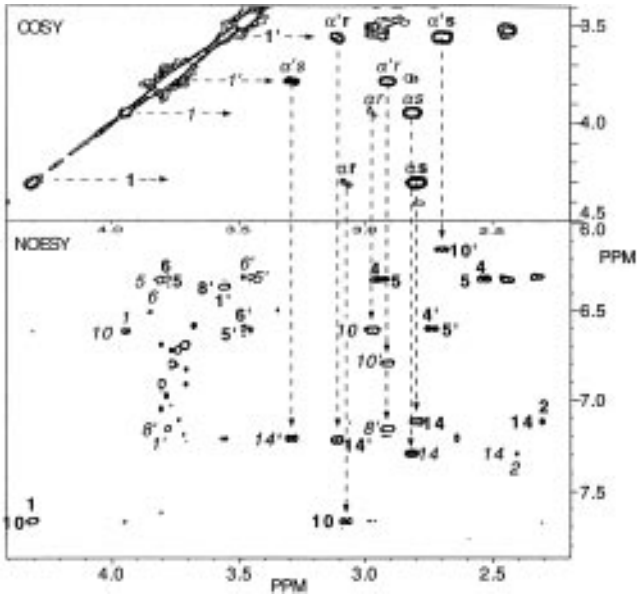

Figure 3. Parts of COSY and related NOESY spectrum of monterine **1** recorded at 275 K and 600 MHz ($CDCl_3$). The COSY panel shows the cross peaks between H1 with Hαs and Hαr; between H1′ with H$\alpha' s$ and H$\alpha' r$ of the major conformer **1a** and the minor one **1b**. The protons of the conformer **1b** are labeled with *italic*. NOESY panel shows the cross peaks of each Hαs and Hαr with the aromatic H10 and H14, respectively, in the benzyl parts of both conformers **1a** and **1b**. H$\alpha' r$**a** signal gives a cross peak with H**14′a**, whereas the equivalent H$\alpha' r$**b** gives cross peaks with H*10′***b** and H*8′***b**. H$\alpha' s$**a** signal gives a cross peak with H**10′a**, the equivalent H$\alpha' s$**b** gives cross peaks with H*14′***b**.

In contrast, the cross peaks located far away from the diagonal indicate the proton resonances most perturbated by interconversion of the two species: $\Delta\delta$H8′ −0.79 (H8′**a**−H8′**b**), $\Delta\delta$H10′ −0.65, and $\Delta\delta$H10 +1.06 for the aromatic part; $\Delta\delta$H$\alpha' s$ −0.60 and one $\Delta\delta$H4′ −0.65 ppm for the aliphatic part.

The stereospecific assignment of α pro*R* (α*r*) and α pro*S* (α*s*)[20] protons is deduced from the observation of the NOEs with the neighboring aromatic protons H10 and H14 and from the 3D structure described below, since the rotation about the Cα−C9 bond is quite limited. The COSY spectrum (275 K) furnished the cross peaks of Hαr, Hαs with H1 and H$\alpha' r$, H$\alpha' s$ with H1′ for the major **1a** and the minor **1b** (labeled with italic) components. The equivalence between these peaks was established as shown previously by observation of negative cross peaks (Figure 2). The benzyl Hαr and Hαs resonances gave positive NOE cross peaks with the aromatic H10 and H14, respectively, in the benzyl parts of both species **1a** and **1b** (Figure 3). In contrast, H$\alpha' r$**a** is close to H14′**a** in the major conformer **1a**, whereas equivalent H$\alpha' r$**b** is close to H*8′***b** and H*10′***b** in the minor one, **1b.** The NOEs were observed between H$\alpha' s$**a** and H10′**a**; H$\alpha' s$-**b** and H*14′***b**. These results led to the conclusion that a D ring inversion does occur during interconversion between **1a** and **1b** by reference to the neighboring methylene group $CH_2\alpha'$. The variation of the ^3J coupling constants between H1′ and H$\alpha' s$; H1′ and H$\alpha' r$, in conformers **1a** and **1b**, corroborates the presence of two distinct rotamers about the C1′-Cα′ bond (Table 1).

Interconversion Rate by Dynamic NMR Studies. Dynamic NMR experiments[13] were carried out with monterine **1** and granjine **3** in pyridine-d_5 at 360 MHz. Coalescences were especially examined with H**1a** at δ 4.53 and H**1b** at δ 4.27 signals: J 7.6 Hz and <1.0 Hz and $\Delta\nu$ 89.9 Hz at 255 K. The observation with monterine **1** of specific 1D NOEs at 275 K by comparison with the nonspecific NOEs observed at 300 K is due to the relative values of relaxation and exchange ($T_1 = R_1^{-1}$ and k_{ex}) at these temperatures (Figure 1).[21] At 275 K, relaxation is much faster than exchange (k_{ex} 0.6 $s^{-1} \ll R_1$ 2.3 s^{-1}); exchange does not affect the NOEs. At 300 K, exchange rate became faster than relaxation rate (R_1 1.6 $s^{-1} < k_{ex}$ 2.1 s^{-1}), and the irradiation energy was transferred to the second equivalent resonance by exchange giving nonspecific NOEs. By raising the temperature of a monterine **1** solution in pyridine-d_5, the exchange rate attained the order of the J-timescale, and the coalescence of J-coupled peaks was first observed producing two broad signals at 355 K ($\Delta\nu$ 85.6 Hz, k_{ex} 64 s^{-1}). The exchange rate still increased with temperature to reach the chemical shift difference timescale, and the two broad signals coalesced at 385 K to furnish a single broad signal. The preliminary coalescence experiments allowed calculation of the free energy of activation according to Eyrings equation (I) substituted with NMR parameters in the range of $\Delta G^{\ddagger}_c$ 77.9 KJ/mol and exchange rate constant at coalescence, k_c 200 s^{-1} for monterine **1** and $\Delta G^{\ddagger}_c$ 77.7 KJ/mol and k_c 211 s^{-1} for granjine **3**.

$$\Delta G^{\ddagger}_c = RT_c[\ln(k/h) + \ln(2^{1/2}T_c/\Pi\Delta\delta)] = 4.575T_c[9.972 + \log(T_c/(\Delta\nu^2 + 6J^2)^{1/2}] \quad \text{(I)}$$

These values are corroborated with the slow exchange system on the NMR timescale at room temperature. This equilibrium is sensible to solvent. The ratio of conformers **a** to **b** can be inverted from $CDCl_3$ to pyridine-d_5 solution. The spectral assignments were ascertained by COSY and NOESY experiments.

(20) IUPAC − IUB Commission on Biochemical Nomenclature. *Biochem. J.* **1971**, *121*, 577.

(21) Neuhaus, D.; Williamson, M. P. *The Nuclear Overhauser Effect in Structural and Conformational Analysis*; VCH Publisher: New York; 1989.

Conformational Analysis by NMR of Monterine 1a and 1b in Solution. Monterine Conformer 1a. Ring current shifts are very important in both conformers **1a** and **1b**. In monterine conformer **1a**, H10′**a** at δ 6.15 and H8′**a** at δ 6.37 are strongly shielded (proton resonance of benzene: δ 7.27) by positive anisotropy[22] of rings C and D, respectively, the two protons lying in the shielding regions of these aromatic rings. Deshielding of H10**a** at δ 7.67 may be due to negative anisotropy of the aromatic rings. Consequently, H10**a** must be located in the plane of the benzene rings, but outside. The NOEs at 275 K indicate spatial proximity of H10**a** to H1**a** (6% NOEs), H8′**a** (4%), and H10′**a** (5%), but NOEs are absent between H8′**a** and the remote H10′**a**, as well as between H10′**a** and H1′**a**, in agreement with rings C and D being approximately parallel, results obtained from analysis of the chemical shifts.

Further support is obtained from measurement of the dihedral angles CH1**a**−CHα*s***a** or CH1**a**−CHα*r***a** and CH1′**a**−CHα′*s***a** or CH1′**a**−CHα′*r***a** estimated by a Karplus type relationship[22,24] from the vicinal proton coupling constant determined on the ^{1}H−^{1}H phase-sensitive COSY[23] spectra: 8 Hz for $^3J_{HH}$ corresponds to a vicinal HH dihedral angle of 25−40° or 140−155°; 10 Hz to 20−35° or 145−155°; <1 Hz to 65−115°.

Accommodating simultaneously all the conformational requirements, i.e. absolute configurations 1*R*,1′*S*, data of anisotropic and NOEs of intracyclic protons, and dihedral angles, the structure of conformer **1a** of monterine (1*R*,1′*S*) was constructed with a Dreiding model. The model revealed pseudoaxial attachment of Cα and Cα′ as well as for *N*-CH$_3$-2 and -2′. The dihedral angle CH1**a**−CHα*s***a** (δ 2.80, $J_{1,\alpha s}$ 8.0 Hz) is about −140°; CH1**a**−CHα*r***a** (δ 3.08, $J_{1,\alpha r}$ < 1.0 Hz) is close to +90°; CH1′**a**−CHα′*s***a** (δ 2.70, $J_{1',\alpha' s}$ 10.2 Hz) is close to −175°; CH1′**a**−CHα′*r***a** (δ 3.11, $J_{1',\alpha' r}$ 5.0 Hz) is approximately +60°. The model thus furnished approximate values for the dihedral angles of the macrocycle: −150° for C8a−C1−Cα−C9 and +60° for C8′a−C1′−Cα′−C9′.

Monterine Conformer 1b. In conformer monterine **1b**, H8′**b** at δ 7.16 is located in the outside anisotropic area of the aromatic rings. H10**b** at δ 6.61 and H10′**b** at δ 6.80 are shielded by the anisotropy of ring C, but not so strongly as H8′**a** and H10′**a** in conformer **1a**. H5′**b** is shielded, too; NOEs at 275 K indicate that H10′**b** is close to H8′**b** (4%).

The vicinal proton coupling constants $^3J_{1',\alpha' s}$ and $^3J_{1',\alpha' r}$ are strongly modified to 3.0 and 4.0 Hz. These values correspond to dihedral angles of approximately 45−60° or 115−130° and 35−60° or 120−145°, respectively. A Dreiding model setting all these NMR data and 1*R*,1′*S* configuration showed dihedral angles of −140° for CH1−CHα*s***b**, +90° for CH1−CHα*r***b**, +100° for CH1′−CHα′*s***b** and −45° for CH1′−CHα′*r***b**. The structure obtained suggests that ring D must be inverted with respect to ring C. The dihedral angles of the macrocycle are −150° for C8a−C1−Cα−C9 and −60° for C8′a−C1′−Cα′−C9′.

Conformation Analysis by Molecular Dynamic Simulation Calculations. Molecular dynamic simulation calculations were performed by a simulated annealing method,[25] *in vacuo*, with distance and angular constraints (Table 3), using the CVFF force field[26] in Insight II/Discover software packages. Five NOE-derived distance restraints of 2−4 Å were applied. Two macrocyclic dihedral angle restraints: −150° ± 30° for C8a−C1−Cα−C9 and + 60° ± 30° for C8′a−C1′−Cα′−C9′ for monterine **1a**; −150° ± 30° and −60° ± 30°, respectively, for conformer **1b**, were also applied. The starting molecule was built on the basis of the Dreiding model conformation and by the CVFF energy minimization with restraints. The restrained structure is then treated with constraints, *in vacuo*, by the simulated annealing procedure at 900 K with a dynamic run for 200 ps. Two hundred structures were sampled during dynamics and cooled to 300 K, and then their coordinates were stored. All the structures were further refined with restraints by the CVFF energy minimization procedure.

Table 3 Angular and Distance Constraints of Monterine Conformers 1a and 1b Used for MD Simulations

conformer **1a**		conformer **1b**	
H10−Hα*r*	2−3 Å	H10−Hα*r*	2−3 Å
H14−Hα*s*	2−3 Å	H14−Hα*s*	2−3 Å
H10′−Hα′*r*	2−3 Å	H10′−Hα′*r*	2−3 Å
H14′−Hα′*s*	2−3 Å	H14′−Hα′*s*	2−3 Å
H3−Hα*s*	2−4 Å	H3−Hα*s*	2−4 Å
C8a−C1−Cα−C9	−150° ± 30°	C8a−C1−Cα−C9	−150° ± 30°
C8′a−C1′−Cα′−C9′	+60° ± 30°	C8′a−C1′−Cα′−C9′	−60° ± 30°

The calculated structures satisfying the NMR criteria with lower overall energy were retained. Figure 4 presents superimposition of 6 lower energy and acceptable structures of conformers **1a**, **1b**, and isogranjine **6**.

The averaged values of the macrocyclic dihedral angles obtained from 200 MD simulated conformations of monterine **1a**, **1b**, and granjine **6** are summarized in Table 4. The dihedral angle[20] of monterine **1a** is +51° for ring B with ring D; +67° for ring A with ring C. The macrocyclic dihedral angles are −143° for C8a−C1−Cα−C9, −88° for C10′−C9′−Cα′−C1′ and +73° for C8′a−C1′−Cα′−C9′. The distances between H1**a** and H10**a**, H10**a** and H10′**a**, H10**a** and H8′**a** are in the range 2.5−2.7 Å, thus corresponding to a close spatial relationship and ring C of conformer **1a** is roughly parallel to ring D.

Dihedral angles of conformer **1b** are −144° for C8a−C1−Cα−C9 and −44° for C8′a−C1′−Cα′−C9′. Ring D is, indeed, bent back toward ring C. This is further corroborated by the fact that the interaction of these near eclipsed conformations is indicated by shielding of the ^{13}C shift of Cα′**b** at δ 36.69 in comparison with Cα**b** at δ 39.61, due to ring strain[27,28] caused by steric repulsions of the inner H8′ and H10′ (2.5 Å). The gauche conformation of C8′a−C1′−Cα′−C9′ of monterine **1a** also produces shielding[28,29] of Cα′**a** at δ 36.89.

Thus, spatial disposition of rings A, B, and C is similar and relatively stable during the dynamic process in both conformers **1a** and **1b**, whereas the main variations affected the dihedral angles C8′a−C1′−Cα′−C9′ and C10−C11−C11′−C10′ which move, respectively, from

(22) Jackman, L. M.; Sternhell, S. *Applications of NMR Spectroscopy in Organic Chemistry*: 2nd ed.: Pergamon Press: New York, 1969.
(23) Neuhaus, D.; Wagner, G.; Vasak, M.; Kägi, J. M. R.; Wüthrich, K. *Eur. J. Biochem.* **1985**, *151*, 257. Marion, D.; Wüthrich, K. *Biochem. Biophys. Res. Commun.* **1983**, *113*, 967.
(24) Karplus, M. *J. Am. Chem. Soc.* **1963**, *85*, 2780. Haasnoot, C. A. G.; Leeuw, F. A. A. M.; Altona, C. *Tetrahedron* **1980**, *36*, 2783.
(25) Nilges, M; Clore, G. M.; Gronenborn, A. M. *FEBS Lett.* **1988**, *229*, 317. Havel, T. F. *Prog. Biophys. Mol. Biol.* **1991**, *56*, 43. Kirkpatrick, S.; Gelatt, C. D.; Vecchi, M. P. *Science* **1983**, *220*, 671.
(26) Dauber-Osguthorpe, P.; Roberts, V. A.; Osguthorpe, D. J.; Wolff, J.; Genest, M.; Hagler, A. T. *Proteins: Struct. Funct. Genet.* **1988**, *4*, 31. Allinger, N. L.;Yuh,Y. H. *J. Am. Chem. Soc.* **1989**, *111*, 8551.
(27) Burke, J. J.; Lanterbur, P. C. *J. Am. Chem. Soc.* **1964,** *86*, 1870.
(28) Dalling, D. K.; Grant, D. M.; Paul, E. G. *J. Am. Chem. Soc.* **1973**, *95*, 3718.
(29) Ritter, W.; Hull, W.; Cantow, H.-J. *Tetrahedron Lett.* **1978**, 3093.

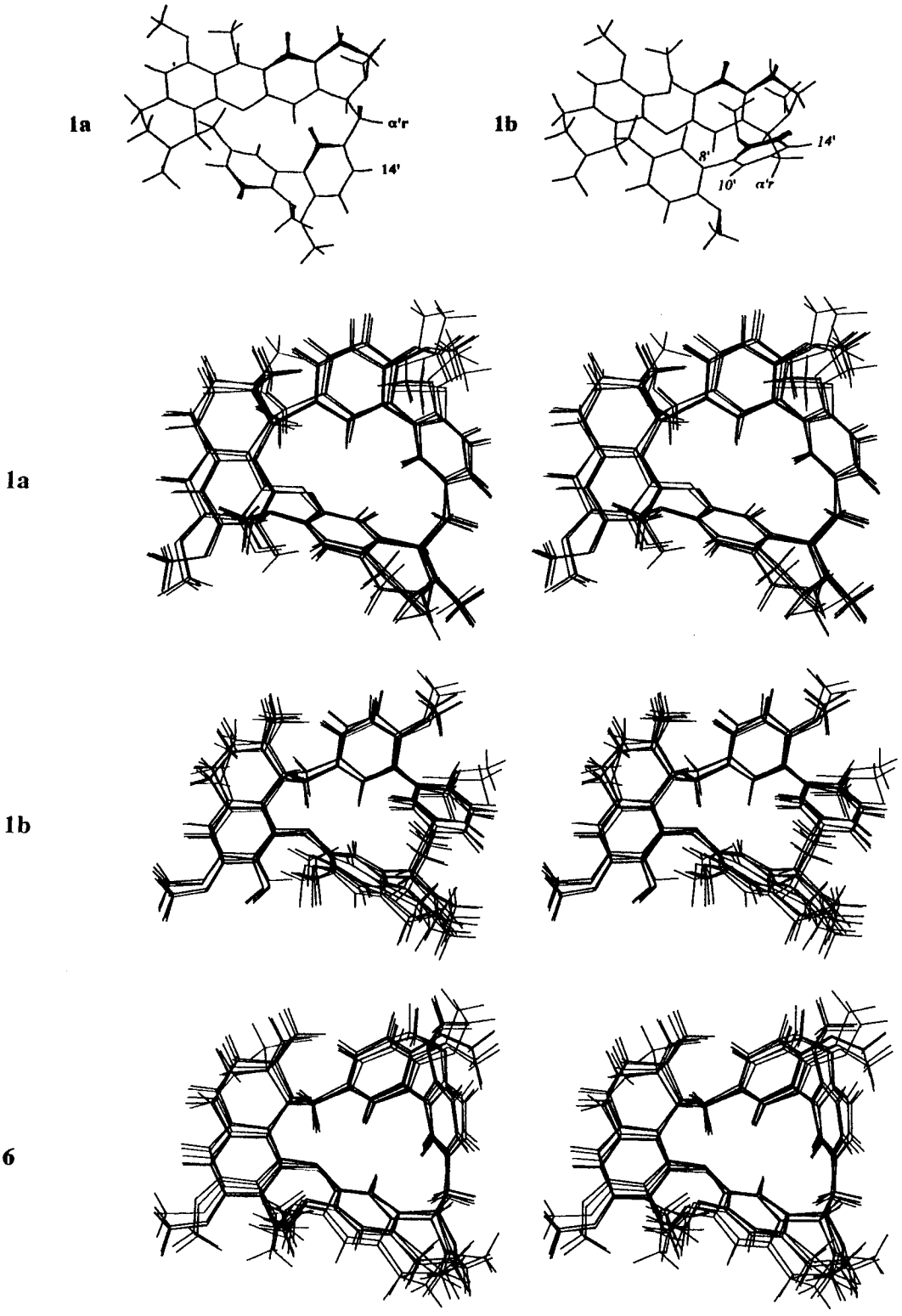

Figure 4. Stereoview of monterine conformers **1a** and **1b** (1*R*,1′*S*) and isogranjine **6** (1*R*,1′*R*) obtained by molecular dynamics simulations. Six structures, of lower overall energy and acceptable for NMR criteria, are superimposed. The figures reveal the mobility of the rings as well as of the *N*-methyl and *O*-methyl groups with respect to the macrocycle.

+73° (**1a**) to −44° (**1b**) and from +51° (**1a**) to −48° (**1b**). The atropisomerism of the biphenylic rings B and D is thus inverted into *aR* in conformer **1b** from *aS* in conformer **1a** with simultaneous −117° rotation around the C1′**b**−Cα′**b** axis. No inversion of rings A and C occurs, and the dihedral angles are +67° in **1a** and +74° in **1b**. Shielding of H5′**b** appears produced by the anisotropy of ring D. Interconversion of the piperidine rings of the isoquinoline moieties is readily observed all over the 200 ps dynamic run (Figure 4). The *N*-methyl groups also oscillate between axial and equatorial position during dynamics. A noteworthy consequence is that quite distinct NOE values were observed, in the 1D NOE experiment, on H1 by irradiation of vicinal *N*-methyl-2 in both species: 13% for conformer **1b** and only 8% for the more mobile conformer **1a**, and H1′ was 6% enhanced by irradiation of the very mobile *N*-methyl-2′ in both conformers. These results clearly indicate that the

Table 4. Dihedral Angles (deg) of MD Simulated Structures[a]

	monterine **1a**	monterine **1b**	isogranjine **6**
C8a−C1−Cα−C9	−143	−144	−144
C1−Cα−C9−C10	+75	+81	+78
C10−C11−C11′−C10′	+51	−48	+50
C10′−C9′−Cα′−C1′	−88	+88	10
C9′−Cα′−C1′−C8′a	+73	−44	−70
C7−C8−C7′−C6′	+67	+74	+66

[a] Averaged values of the macrocyclic dihedral angles were obtained from 200 structures calculated by MD simulations during a dynamic run over 200 ps at 900 K.

interconversion between **1a** and **1b** involves three significant rotations about the C1′−Cα′, Cα′−C9′ and C11′−C11 bonds. The rather bulky 12- and 12′-methoxyl groups of the biphenyl moiety, in 1*R*,1′*S* configured monterine, slow down the rate of the interconversion thus producing two highly populated conformations at room temperature. These facts are well defined by NMR analysis through the observation of coupling constants, anisotropic shielding, and NOEs. The molecular dynamics studies corroborated the mobility of molecules and clarify the strong flexibility of conformer **b**.

In the case of granjine, conformer **3a** is more stable than **3b** (ratio: 70:30). The dihedral angle for C8a−C1−Cα−C9 is −144° in **3a** and in **3b**; C8′a−C1′−Cα′−C9′ is +78° in **3a** and −42° in **3b**. The 7-methoxyl group may reduce the flexibility of the C8−O−C7′ axis and render inversion of ring D more difficult. ^{13}C shielding of C4 near δ 22 is a result of γ effect[28] between pseudoaxial *N*-CH_3-2 and pseudoaxial H4.

The stereoisomer of **1**, 1*R*,1′*R* configured isogranjine **6**, obtained by MD simulation procedure, has only one type of spirallike structure as drawn in Figure 4. Dihedral angles are −144° for C8a−C1−Cα−C9, −70° for C8′a−C1′−Cα′−C9′, +50° for rings B and D, and +66° for rings A and C. Deshielding of H10 near δ 7.6 is induced by the negative anisotropy of rings A and C. H10′ is shifted to higher field by the aromatic ring C. Cα is pseudoaxial, and Cα′ is pseudoequatorial. The 6′-methoxyl proton signal is strongly shielded by the anisotropy of ring A.

The aromatic and methoxyl shifts, affected by anisotropy (*vide supra*), proved of high diagnostic value in the biphenylic bisbenzylisoquinolines with one ether linkage,[30] allowing the relative configuration to be defined as 1*R*,1′*R* (or 1*S*,1′*S*): δ 6.40−7.60 and δ 7-OMe > δ 6′-OMe or 1*R*,1′*S* (or 1*S*,1′*R*): δ 6.35-7.35 and δ 7-OMe < δ 6′-OMe, except for monterine **1**, granjine **3**, and dimethylantioquine.[10]

Cytotoxic Activity. Cytotoxicity of biphenyl bisbenzylisoquinolines was measured *in vitro*[31] on three human tumor cell lines: prostate cancer (PC3), breast adenocarcinoma (MDA-MB 231), and breast cancer (MCF 7) (Table 5). The 1*R*,1′*S* configured alkaloids (five compounds) and the 1*R*,1′*R* ones (four compounds) displayed a similar range of cytotoxic responses: IC_{50} value are 1.6−7.7 μg/mL against three cell lines. Hence, C-1*R* configured moiety and ring C in similar spatial arrangement are likely to be significant for cytotoxic activity of C8−O−C7′ bridged biphenylic bisbenzylisoquinolines.

Table 5. Cytotoxic Activity *in Vitro* of Biphenylic Bisbenzylisoquinoline Alkaloids

compound	cell line (IC_{50} μg/mL)[a] PC3	MDA-MB231	MCF7
monterine **1**: 1*R*,1′*S*	3.95	2.03	3.44
7-methylcordobine **2**: 1*R*,1′*S*	2.95	ND	3.76
granjine **3**: 1*R*,1′*S*	4.76	2.81	4.89
dihydrocordobimine: 1*R*,1′*S*[14]	3.44	ND	ND
cordobimine[14]: 1*R*	1.88	1.79	2.09
dihydrocordobimine: 1*R*,1′*R*[14]	3.75	2.02	3.53
epicordobine **4**: 1*R*,1′*R*	3.13	1.62	4.98
epirodiasine **5**: 1*R*,1′*R*	4.72	2.04	5.92
isogranjine **6**: 1*R*,1′*R*	2.67	2.76	3.64
cordobine **7**: 1*R*,1′*S*	5.27	2.33	7.69
antioquine: 1*S*,1′*R*[10]	>10	>10	>10
doxorubicine	0.05	0.05	0.02

[a] PC3: Human prostate cancer; MDA-MB231: human breast adenocarcinoma; MCF7: human breast cancer; ND: not determined.

Moreover, some bisbenzylisoquinolines, *e.g.* tetrandrine, cepharantine, and 2-*N*-methyltelobine, were able to reverse vinblastine-promoted multidrug-resistance of cancer cells.[32] The alkaloids mentioned in this report are under investigation as potential agents against multidrug-resistant tumor cell lines.

Conclusion

In the group of 11,11′-biphenylic and C8−O−C7′ etherlinked bisbenzylisoquinolines, endowed with 1*R*,1′*S* (or 1*S*,1′*R*) configuration, monterine **1** and granjine **3** generate two highly populated conformers, due to atropisomerism produced by steric hindrance of the 12- and 12′-methoxyl groups. The alkaloids **1** and **3** thus display two sets of NMR signals. Interconversion of both conformers was detected by saturation transfer in 1D and 2D ^{1}H NMR NOE experiments. This slow exchange system on the NMR timescale displayed a coalescence at 385 K; free energy of activation and exchange rate constant at coalescence were determined by dynamic NMR: $\Delta G_c^{\ddagger}$ 77.9 KJ mol^{-1}, k_c 200 s^{-1} for monterine **1**; $\Delta G_c^{\ddagger}$ 77.7 KJ mol^{-1}, k_c 211 s^{-1} for granjine **3**, respectively.

The moiety implicated in interconversion of these macrolides, monterine **1** and granjine **3**, demonstrated the change of $^3J_{HH}$ coupling constants and of NOEs as well as variation of aromatic ring anisotropies. The molecular dynamics simulation calculations *in vacuo* of two highly populated conformers indicate the flexible part of the conformations. These results clearly establish that two highly populated conformers, monterine **1a** and **1b**, as well as granjine **3a** and **3b**, are interconverted by inverting ring D toward ring C with simultaneous inversion of atropisomerism between rings B and D involving rotation about the C1′−Cα′, Cα′−C9′, and C11′−C11 bonds. This would imply slowing down of interconversion rate due to bulky 12- and 12′-methoxyl groups. The methoxyl-7 group in granjine **3** changes the equilibrium, enhancing the **3a** population. The spatial arrangement of the three aromatic rings A, B, and C in monterine **1**, granjine **3**, and isogranjine **6** is similar, as are the cytotoxicities against the human tumor cell lines investigated. All the CH_3O-, HO-, and -*N*-CH_3 groups in the three alkaloids are oriented toward the surface of the molecule, thus producing possible attractive sites for

(30) Berthou, S.; Jossang, A.; Guinaudeau, H.; Leboeuf, M.; Cavé, A. *Tetrahedron* **1988**, *44*, 2193.

(31) Mosmann, T. *J. Immunol. Methods* **1983**, *65*, 55. Carneiro Do Nascimento, S.; Nebois, P.; Benameu, L.; Boitard, M.; Bartoli, M. H.; Fillion, H. *Pharmazie* **1994**, *49*, 296.

(32) Van Dyke, K. U.S. Pat. 5,025,020; *Chem. Abstr.* **1991**, *115*, 105992w. Likhitwitayawuid, K.; Angerhofer, C. K.; Cordell, G. A.; Pezzuto, J. M. *J. Nat. Prod.* **1993**, *56*, 30.

biological targets. Three major cavities are also formed, likely to complex metal ions.

These investigations should be extended to the other bisbenzylisoquinoline structural groups for conformational analysis, allowing structure modifications to be determined in order to improve the important capability and search the biological target of reversing multidrug-resistance of cancer cells, a crucial problem in oncology.

Experimental Section

General Methods. ^{1}H and ^{1}H−^{1}H COSY spectra, proton NOEs, and saturation transfer experiments were performed in $CDCl_3$ on Bruker AMX 360 and AMX 600 spectrometers (360 and 600 MHz), referenced to TMS ($\delta = 0$). ^{1}H NOE difference spectra and saturation transfer experiments were acquired automatically by using both on- and off-resonance spectra. The decoupler was cycled through series of frequencies chosen with irradiation (5−6 s, power attenuation 55 L), resulting in efficient saturation at low decoupler power levels. Difference spectra were obtained in the FID stage prior to Fourier transformation by substraction of the control (off-resonance irradiation) from each other spectrum. ^{13}C and ^{13}C−^{1}H COSY spectra were recorded on a Bruker AC-300 spectrometer (^{1}H: 300.13 MHz, ^{13}C: 75.45 MHz) using Bruker pulse sequences. The HMBC spectrum was optimized for J_{CH} 7.14 Hz. The NOESY spectra, recorded at 600 MHz on a Bruker AMX 600 spectrometer, were performed with 1 s relaxation delay, 40 ms mixing times, and apodization with a shifted sine bell and base line corrections.

Molecular Dynamics Simulation Calculations. The simulated annealing method was performed with the INSIGHT II/DISCOVER software packages (version 2.1) using the CVFF force field (Biosym Technologies, 10065 Barnes Canyon Rd., San Diego, CA 92121) on Silicon Graphics-4D/30 work station. The starting molecules were manually built on the basis of the Dreiding model conformation with the INSIGHT II (Biosym) molecular graphics program and energy minimized. The MD simulations were carried out *in vacuo*. The simulations started with the experimental distance restraints (lower distances were bound set to 2 Å and the upper ones to 3 and 4 Å). The distance restraints were applied using a force constant of 15 kcal mol^{-1} Å^{-2}. Two macrocyclic dihedral angle restraints: −150° ± 30 for C8a−C1−Cα−C9 and + 60° ± 30 for C8′a−C1′−Cα′−C9′ for monterine conformer **1a**; −150° ± 30 and −60° ± 30, respectively, for conformer **1b**, were also applied with a force constant of 200 kcal mol^{-1} rad^{-2}. A simulated annealing procedure was then applied: the temperature was rised to 900 K by steps of 300 K, and dynamics were allowed to run for 200 ps, *in vacuo*, by the steepest descent algorithm method for 1 ps (1.0 fs timestep), followed by full optimization with enough conjugate gradient iterations for 1 ps to reach the root mean square of the gradients which was 0.001 kcal Å^{-1}. Coordinate sets of 200 structures were sampled every 1 ps and cooled to 300 K. The structures were then energy minimized with constraints by the CVFF force field procedure. The calculated structures satisfying the NMR criteria and acceptable with lower overall energy were retained.

Methylcordobine 2. A solution of **7** [14] (10 mg) in 0.5 mL of MeOH was treated 24 h at 20 °C with 10 mL of diazomethane in ether solution. The dry residue furnished 10 mg of **2**, amorphous, $[\alpha]^{20}_D$ −150° ($CHCl_3$, *c* 1.0), ^{1}H, ^{13}C NMR ($CDCl_3$, Tables 1 and 2), CIMS *m*/*z* (rel intensity) 623 ([MH]$^+$, 100), 621 (25), 396 (23), 395 (30), 381 (15), 198 (12), 176 (34).

Epicordobine 4. Dihydrocordobimine 1′*R*[14] (100 mg) in MeOH (2 mL) was allowed to react at 20 °C for 30 min with 30% HCHO (0.5 mL) and reduced by $NaBH_4$. CH_2Cl_2 extraction from the reaction mixture in aqueous ammonia and then SiO_2 column chromatography provided 95 mg of alkaloid **4**, mp 188−189 °C (MeOH), $[\alpha]^{20}_D$ −31° ($CHCl_3$, *c* 1.0), ^{1}H, ^{13}C NMR ($CDCl_3$, Tables 1 and 2), CIMS *m*/*z* (rel intensity) 609 ([MH]$^+$, 100), 607 (15), 382 (20), 381 (24), 191 (21).

Epirodiasine 5. A solution of **4** (30 mg) in 0.5 mL of MeOH was treated 24 h at 20 °C with 10 mL of CH_2N_2−Et_2O. TLC purification of the dry residue furnished 30 mg of **5**, amorphous, $[\alpha]^{20}_D$ −90° ($CHCl_3$, *c* 1.0), ^{1}H, ^{13}C NMR ($CDCl_3$, Tables 1 and 2), CIMS *m*/*z* (rel intensity) 623 ([MH]$^+$, 100), 396 (14), 395 (20), 381(10), 198 (15), 176 (20).

Isogranjine 6. A solution of **4** (30 mg) in 6 mL of MeOH was treated 24 h at 20 °C with 10 mL of CH_2N_2−Et_2O. TLC purification of the dry residue furnished 30 mg of **6**, amorphous, $[\alpha]^{20}_D$ −98° ($CHCl_3$, c 1.0), ^{1}H, ^{13}C NMR ($CDCl_3$, Tables 1 and 2), CIMS *m*/*z* (rel intensity) 637 ([MH]$^+$, 100), 635 (18), 395 (25), 381(10), 198 (21).

Cytotoxicity Assays. The biological evaluations of cytotoxic activities of the compounds were carried out according to established protocols.[31]

Acknowledgment. We are grateful to our colleagues Drs F. Trigalo (Muséum) and T. Alattia (CBS Montpellier) for valuable discussions on structural calculations and Dr J. P. Brouard (Muséum) for mass spectrometry.

Supporting Information Available: ^{1}H and ^{13}C NMR spectra of compounds **1**−**6**; negative NOESY low-field spectrum of monterine **1** (δ 6.1−7.8) recorded at 300 K; temperature evolution of H1**a** and H1**b** on the ^{1}H NMR spectra of monterine **1** in pyridine-d_5 at 360 MHz and stereoview of the lowest overall energy structures of monterine conformers **1a** and **1b** and isogranjine **6** calculated by molecular dynamics simulations (15 pages). This material is contained in libraries on microfiche, immediately follows this article in the microfilm version of the journal, and can be ordered from the ACS; see any current masthead page for ordering information.

JO950767N